Thermal and structural analysis of the DONES target system under steady state and transient loading conditions

I. Catanzaro [a,*], P. Arena [b], D. Bernardi [b], G. Bongiovì [a], T. Dezsi [c,d], P.A. Di Maio [a], F.S. Nitti [b], S. Giambrone [a], M. Giardina [a], S. Gordeev [e], A. Quartararo [a], E. Tomarchio [a], E. Vallone [a]

[a] Department of Engineering, University of Palermo, Viale delle Scienze, Ed. 6, 90128, Palermo, Italy
[b] ENEA, Department of Fusion and Nuclear Safety Technology, C.R. Brasimone, 40032, Camugnano, BO, Italy
[c] Centre for Energy Research (EK-CER), Budapest, Hungary
[d] C3D Engineering Consultant Ltd., Hungary
[e] Karlsruher Institut für Technologie, Campus Nord, Eggenstein-Leopoldshafen, Germany

ARTICLE INFO

ABSTRACT

One of the crucial steps in the European Roadmap to the realisation of fusion energy is the design and construction of the Demo-orientated NEutron Source (DONES) facility. DONES is a fusion-like neutron source, based on the International Fusion Materials Irradiation Facility (IFMIF) concept, aimed at qualifying and testing the materials to be used in fusion reactors. The Target System (TSY) is a crucial system as it is the component where the interactions between deuterons and a liquid lithium target, flowing on a solid surface (i.e. the Back Plate), take place to produce neutrons for irradiating the testing materials. In this regard, an investigation campaign has been performed to evaluate the thermo-mechanical behaviour of the DONES TSY under selected steady state and transient loading conditions, in light of the most recent design updates (new bellows and connection systems). The first part of the assessment concerned the analysis of the TSY under the normal operation steady state loading scenario. A detailed 3D FEM model has been set up, considering the newest updates of the TSY geometry and of the operational parameters, and a thermo-mechanical analysis has been launched. Results have been mainly checked in terms of TSY global deformation, focusing on the Back Plate and on the connecting bellows displacements, in order to exclude overlapping with the High Flux Test Module and misalignments with the beam footprint. Afterwards, since the lithium inlet temperature has been increased from 250 °C to 300 °C, a transient thermo-mechanical analysis of the TSY under the start-up loading conditions has been performed to check if it is able to withstand the hotter lithium flow according to the RCC-MRx criteria. Therefore, the reference pre-heating strategy has been adopted, assessing the thermal and mechanical behaviour of the TSY, focusing on the Back Plate. The obtained results are presented and critically discussed, suggesting important recommendations for the follow-up of the design.

1. Introduction

In order to test and qualify materials in a proper fusion environment, the EUROfusion consortium is making a great effort to design the DEMo orientated NEutron Source (DONES) facility, based on the International Fusion Materials Irradiation Facility (IFMIF) concept [1–3]. In this regard, a crucial aspect is represented by the design of the Target System (TSY), whose Back Plate (BPL) is devoted to house the deuterons-lithium nuclear interactions aimed at the neutrons production. Hence, the work herein presented concerns the assessment of the thermo-mechanical

performances of the TSY under selected steady state and transient loading conditions.

In the first part, the thermo-mechanical behaviour of the up-to-date version of the DONES TSY under the steady state conditions related to the beam-on nominal operational phase has been assessed. The main scope has been the evaluation of the DONES TSY arising displacement field in order to qualify its design. On the one hand, the maximum BPL displacement towards the High Flux Test Module (HFTM), which contains the irradiated materials, has been checked. On the other hand, the relative displacements of the bellows flanges connecting the Beam Ducts

---

* Corresponding author.
E-mail address: ilenia.catanzaro@unipa.it (I. Catanzaro).

(BDs), which transports the deuteron beam, and the Quench Tank (QT), which collects the Li jet, to the structure including the BPL, namely the Target Assembly (TAA), has been evaluated.

In the second part, attention has been paid to the start-up transient scenario [4], consisting in the pre-heating and lithium injection phases, in order to verify whether the TSY can safely withstand the corresponding set of loads and boundary conditions, in compliance with the RCC-MRx structural design criteria [5]. Moreover, attention has been paid to the BPL lithium channel temperature, in order to check if the thermal field achieved at the end of the pre-heating phase is enough to guarantee that the lithium temperature upon injection remains above ~200 °C, allowing to reasonably exclude its local solidification and avoid excessive thermal stresses in the structure.

The whole study has been performed following a theoretical-numerical approach based on the Finite Element Method (FEM) and adopting the quoted ABAQUS v. 2022 commercial code [6].

2. The dones target system

The DONES TSY is aimed at generating and maintaining a neutron flux to irradiate the material samples placed in the HFTM, which is located behind it. Neutrons are generated thanks to the nuclear interactions between an accelerated deuterons beam and a free-surface high-speed jet of liquid lithium flowing in front of it.

The DONES TSY is mainly composed of the TAA (in pale grey in Fig. 1), the lithium piping (in pale blue and dark grey in Fig. 1), the BDs (in orange in Fig. 1), the TAA support structure (in green in Fig. 1) and the QT (in purple in Fig. 1). In Fig. 1 the connection points with the Test Cell-Lithium System Interface Cell (TLIC), namely at the upper surface of the lithium inlet pipe bellow and at the lithium inlet pipe flange, are reported. Moreover, a layer of insulation covers the Lithium Inlet Pipe, Inlet Nozzle, Target Vacuum Chamber and Outlet Nozzle (excluding the bellow).

The core of the TSY is represented by the TAA, where the neutron production reactions take place in the lithium footprint region, located in correspondence of the centre of the BPL. A detailed description of the TSY can be found in [3]. Here, it has to be recalled that the TAA arms are connected to the HFTM by means of a complex hinge mechanism, an initial nominal gap of 2 mm is present between the BPL and the HFTM, and the TAA is connected to the BDs and the QT by means of bellows.

3. TSY steady state thermo-mechanical analysis

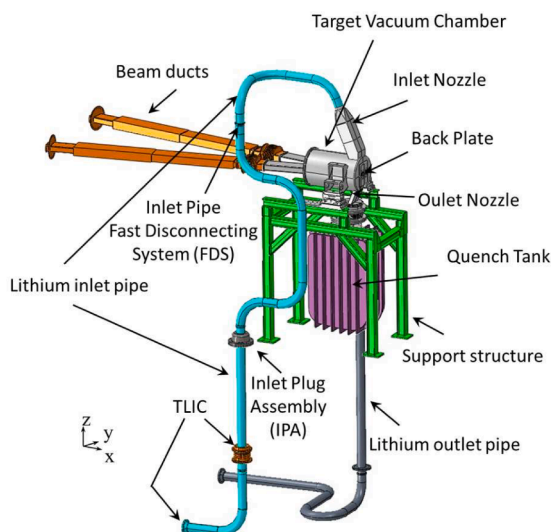In order to assess the steady state thermo-mechanical behaviour of

Fig. 1. The DONES Target System.

the DONES TSY, uncoupled thermal and mechanical analyses has been carried out adopting the most recent geometric configuration of the TSY.

3.1. Thermal analysis: the 3D fem model

A 3D FEM model reproducing the DONES TSY, considering the TAA and its support structure, the BDs, the lithium inlet pipe and the lithium flowing on the BPL and the ON channel (which drives the Li jet to the QT) has been set up. The QT, the Outlet pipe and the lithium flowing elsewhere have not been modelled, being their presence simulated by means of proper thermal loads and boundary conditions.

With respect to the previous TSY models, the following updates have been introduced:

- refinement of the spatial discretization grid and revision of some of the implemented thermal and mechanical contact models;
- implementation of the new bellows selected for the BDs and ON;
- HFTM expected average temperature;
- implementation of new TAA arms geometry to consider the TAA-HTFM attachment system;
- 3D spatial distribution of the neutronic and photonic volumetric power density deposited within TAA, lithium, support structure, pipes and bellows;
- lithium inlet temperature increased from 250 °C to 300 °C;
- Test Cell (TC) atmosphere pressure and Lithium centrifugal pressure;
- revision of the Lithium pressure within the pipes and inlet nozzle;
- revision of the Lithium pressure onto the BPL;
- ON, inside the QT, partially immersed in Lithium at 318 °C;
- imposed QT flange temperature and displacement;
- revision of thermal and mechanical restraints.

A mesh composed of ~2.3 M nodes connected in a mix of ~2.8 M linear tetrahedral and hexahedral elements has been obtained for the thermal model. It has to be observed that the bellows connecting the TAA to the BDs and to the QT have been modelled too, in order to take into account their influence on the TSY thermal behaviour.

As to the structural materials, the RAFM Eurofer steel has been assumed for the TAA and the first part of the inlet pipe (from the inlet nozzle to the Inlet Pipe FDS), whereas the AISI 316 L steel has been assumed for all the other components. All the materials, including lithium, have been considered as homogeneous, uniform and isotropic and their temperature-dependant thermophysical properties have been implemented. The physical property of Eurofer [7], AISI316L [8,9] and Lithium [10–12] have been assumed.

In order to realistically investigate the thermal behaviour of the DONES TSY under the normal operation steady state loading scenario, the following loads and boundary conditions, pertaining the beam-on phase, have been considered in view of the most recent updates:

- volumetric density of nuclear heat power deposited within lithium beam footprint region by deuterons;
- volumetric density of nuclear heat power deposited within lithium and structural materials by neutrons and γ;
- thermal contacts modelling;
- lithium flow convective heat transfer;
- external and internal TAA uninsulated surfaces heat transfer;
- imposed temperatures.

A uniform power density of 2.0E+10 W/m^3 has been calculated and imposed to the elements in red in Fig. 2, to consider the 5 MW power deposited by the deuterons beam within the 20×5 × 2.5 cm^3 vol of the Li footprint.

The 3D non-uniform spatial distribution of nuclear heat power deposited within lithium and structural materials [13] has been mapped and applied to the FEM model. Details of the BPL are depicted in Fig. 3.

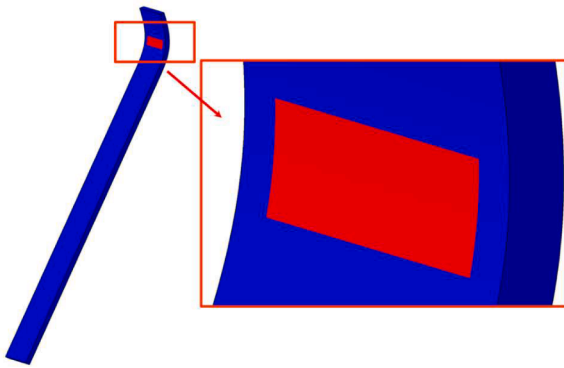A thermal contact model characterised by a thermal conductance of

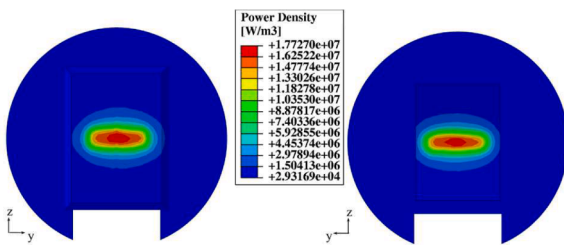**Fig. 2.** Lithium flow domain beam footprint region.

Fig. 3. Nuclear power density 3D field within the two sides of the BPL.

2000 W/m² °C [14,15] has been imposed in order to consider the heat transfer between the TAA lateral arms and its support structure. The bellows have been represented as 3D components in the thermal analysis, so to properly assess the heat diffusion between the flanges.

The lithium flowing through the Inlet Pipe and Inlet Nozzle has not been modelled and, therefore, the forced convective heat transfer within these two components has been simulated imposing onto the wetted surfaces a convective heat transfer condition, assuming a lithium bulk temperature equal to 300 °C and a heat transfer coefficient equal to 34,000 W/m²· °C [15,16]. Instead, the Li flow onto BPL and ON has been modelled using 3D forced convection elements, chosen from the Abaqus library. An inlet temperature of 300 °C and a mass flow rate per unit area equal to 7650 kg/(m²·s), obtained assuming a lithium flow velocity of 15 m/s, have been assigned to its boundary nodes. Hence, assuming a uniform heat transfer coefficient equal to 34,000 W/m²· °C [16], the heat transfer between the lithium flow and the BPL and ON channels, characterised by a lithium bulk temperature changing along the lithium flow path, has been taken into account. To this purpose, a proper subroutine has been coded to follow the curvature of the lithium channel.

A radiation cavity has been considered amongst the internals of the Target Vacuum Chamber (TVC), which connects the beam duct with the BPL, the ON and the lithium free surface, imposing emissivity values of 0.3 for Eurofer and 0.06 for Li [17,18]. Moreover, the external thermal radiation and the natural convective heat transfer condition have been applied onto the TSY uninsulated surfaces. Since inside the BDs there is the vacuum, those surfaces are adiabatic. The latter have been considered radiating towards the TC walls, which contains the TSY, assumed at a temperature of 50 °C, with an emissivity of 0.3. In addition, heat transfer coefficients ranging from ~1.0 to ~2.7 W/(m²· °C) calculated by means of Churchill and Chu correlation [19], and a bulk temperature of 50 °C [15,20] have been imposed onto these surfaces to simulate the natural convection with the TC atmosphere. Finally, the thermal interaction between the BPL and the HFTM has been simulated considering a purely diffusive heat transfer through the narrow thickness of the interposed helium gap, characterised by a not-uniform thermal conductance equal to λ/d, where λ is the helium thermal conductivity at 10 kPa [20] and 200 °C [21] and d is the gap amount (ranging from 2 to

25 mm) as already done in [15]. A bulk temperature of 50 °C has been considered.

Since the ON is partially immersed in the lithium within the QT at 318 °C, this temperature has been imposed to the ON nodes of the immersed region [22,23]. Furthermore, the ending regions of the BDs have been assumed at 50 °C, to reproduce their contact with the TC walls. Finally, to realistically simulate the presence of the QT at the bottom part of the TAA, a temperature 3D spatial distribution has been imposed to the flange, depicted in Fig. 4, obtained purposely by mapping the results of a separate thermal analysis [24].

3.2. Thermal analysis: results

Looking at the thermal field obtained from the thermal analysis within the whole TSY (Fig. 5), it can be stated that the maximum achieved temperature is well below the Eurofer suggested limit, equal to 550 °C. The predicted maximum temperature is obtained within the TVC and results equal to about 385 °C. Moreover, the maximum temperature within the BPL (Fig. 6), approximately equal to 350 °C, is obtained in the side region, near lithium flow channel. As it can be observed, the temperature distribution is quite asymmetric, due to the beam inclination of 9° generating a power deposition laterally shifted with respect to the centre of the footprint, as it can be observed in Fig. 3.

3.3. Structural analysis: the fem model

In order to perform the structural assessment of the DONES TSY under nominal conditions, a mesh composed of ~690k nodes connected in ~1.8 M linear tetrahedral and hexahedral elements has been set-up. This difference with respect to the thermal FEM model is due to the fact that, for the mechanical analysis, the bellows, the lithium and the QT connection flange have been removed since their mechanical effect has been simulated by means of the imposition of proper connector elements and boundary conditions.

Hence, the following set of loads and boundary conditions, has been considered:

- thermal expansion;
- gravity load;
- TSY internal and external pressure;
- mechanical contacts modelling;
- mechanical restraints;
- buoyancy forces onto the ON;
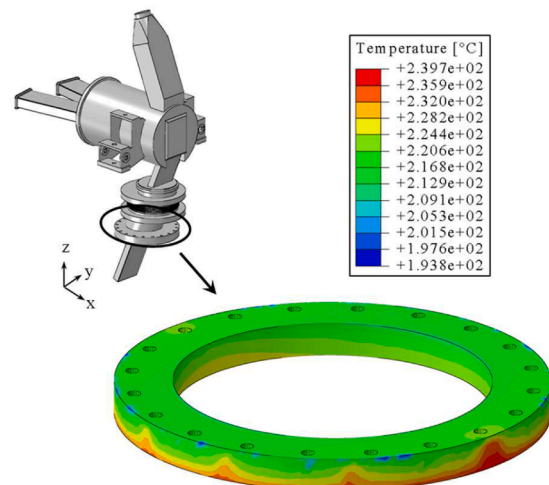- BDs and ON bellows implementation.
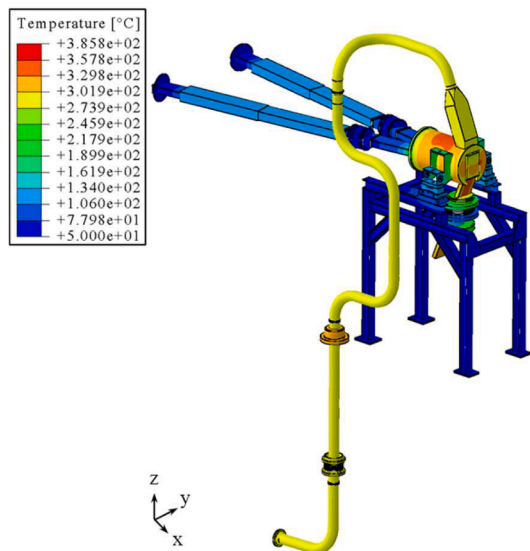

Fig. 4. Imposed temperature of the flange.

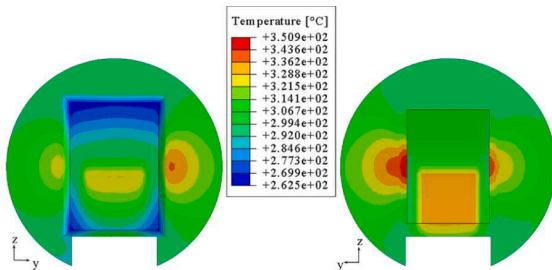**Fig. 5.** Thermal field within TSY.

Fig. 6. Thermal field within the two sides of the BPL.

The non-uniform 3D thermal deformation field obtained from the thermal analysis is applied to the TSY structure.

The acceleration of gravity along the global Z direction has been defined to consider the TSY weight.

In order to simulate the presence of the lithium flowing within the structure, different values of pressure have been applied. In particular, onto the lithium-wetted surfaces of the inlet pipes a pressure of ~0.32 MPa has been applied whereas, at the inlet nozzle internal surfaces, a pressure of ~0.29 MPa has been considered [25]. Furthermore, a 3D spatial distribution of lithium static pressure onto double reducer nozzle and BPL surfaces calculated in [23], has been mapped and applied, as reported in Fig. 7. As it can be observed, the lithium pressure vanishes as it enters the ON and, therefore, the lowest value has been then propagated.

A pressure of 10 kPa [20] has been imposed onto the TSY external uninsulated surfaces in order to consider the inner pressure of the TC atmosphere during normal operation.

The mechanical interaction between the TAA lateral arms and its support structure, considered as dry lubricated, has been modelled by means of a mechanical contact model characterized by a uniform friction factor of 0.03 imposed onto the flat surfaces in contact. Instead, a friction factor of 0.74 has been assumed to simulate the contact in between the connecting pins and the holes [15,18].

In order to take into account the effect of the bolts connecting vertically the TAA arms and the support structure, a kinematic coupling condition along the Z direction has been imposed to a dedicated node set. Furthermore, all the displacements of the nodes lying on the bottom surfaces of the support structure feet have been prevented. The same restraint has been considered in correspondence of the lower surfaces of
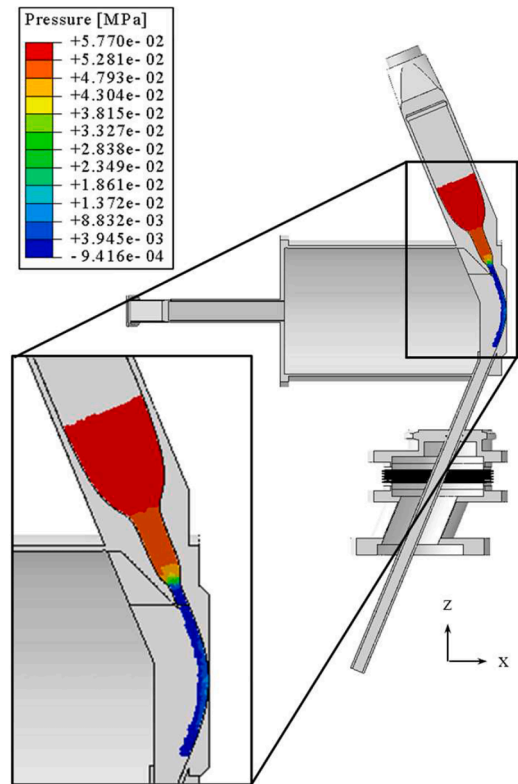

Fig. 7. Lithium static pressure spatial distribution.

the Inlet Plug Assembly (IPA, see Fig. 1), to take into account the connection with the TC floor and at the upper surface of the bellow of the lithium inlet pipe and at the lithium inlet pipe flange, to simulate its fixed junction with the TLIC. All the displacements have been prevented on the nodes at the end of the BDs too to reproduce their fixed connection with the TC walls. In addition, the effect of the TAA-HFTM connection system [26] has been also considered. In fact, the HFTM, connected to the TAA thanks to a complex hinge system acting on the TAA arms, transmits to the TAA along the x direction a resultant force of ~8.4 N [26], calculated from the HFTM mass and centre of gravity location. Therefore, a force, has been applied along the x direction onto nodes lying on the upper surfaces of the TAA arms. Lastly, with the aim of considering the presence of the QT, the displacement fields (u_x, u_y, u_z) [24], have been mapped and imposed at the nodes of the TAA flange lower surface, at the interface with QT, as reported in Fig. 8

In order to reproduce the effect of the buoyancy forces acting on the ON region immersed in QT, an Eurofer equivalent density, calculated starting from the balance between the weight force and Archimedes' force, has been applied to the corresponding elements.
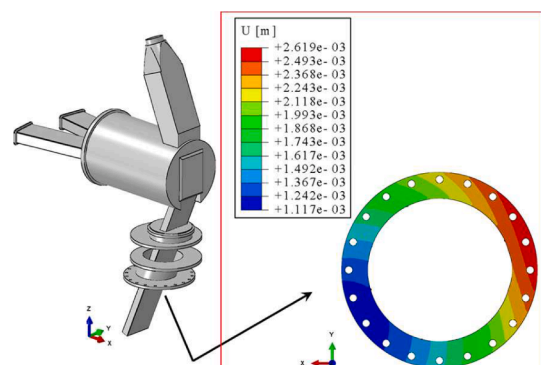

Fig. 8. Imposed total displacement field applied onto the QT flange.

Finally, the bellows located at the BDs and the ON, modelled as 3D components in the thermal analysis, have been simulated in the mechanical analysis by replacing them with springs characterized by proper stiffness, as reported in Figs. 9 and 10.

3.4. Structural analysis: results

The total displacement field (U) within the TSY structure is reported in Fig. 11. As it can be observed, the maximum displacements are obtained at the lithium inlet pipe, with a maximum value of ~1.7 cm, and within the BDs, with a maximum displacement of ~1.3 cm. As to the latter, the obtained results clearly indicate the necessity to integrate into the FEM model proper supports to sustain the BDs.

In addition, paying attention to the BPL displacements and, in particular, to the displacements along the x direction of the BPL surface closest to the HFTM (Fig. 12), the maximum displacement of the face closest to the HFTM is ~1 mm, whereas the BPL central node u_x displacement is less than that. This outcome allows concluding that the contact between them should be excluded but this can be confirmed only with an integrated model.

Results in terms of displacements of the BDs and ON bellows have been also checked. In particular, the relative displacements ΔU_i, with i being the X, Y or Z direction, between the flanges connected by the bellows have been calculated as U_{i1} minus U_{i2}, where flange 1 is on the BD side for Y_{neg} and Y_{pos} (with respect of the y direction, considering the reference system located at the centre of the domain) bellows and on the ON side for the ON bellow, whereas flange 2 is on the TAA side in both cases. Along the bellows' axial directions, the positive sign of ΔU indicates that the bellow is shortened of a quantity equal to ΔU, whereas the negative sign means that the bellow is extended. Instead, as to the transverse directions (i.e. Y and Z for the BD bellows, X and Y for the ON one), any relative displacement generates a transverse extension (i.e. a misalignment of the flanges) of the bellow. Therefore, the modulus $|\Delta U|$ is reported.

Results are reported in Table 1, referring to the local coordinate system of each bellow (using γ for the axial direction and θ_1 and θ_2 for the lateral ones). As to BDs bellows, a compression along the axial direction of ~10 mm is expected whereas a relative displacement of ~15 mm have been calculated along the lateral one corresponding to the Z direction of the global coordinate system. This outcome confirms the necessity to include in the model a proper support to vertically sustain the BDs. As to the ON bellow, whose relative displacements between the connected flanges are reported in Table 1, small relative displacements along the lateral directions have been obtained whereas the resulting relative axial displacement shows that the bellow extends of about 1 mm.

Finally, attention has been paid to the ON region inside the QT, in order to investigate whether it hits the QT inner walls. Since a maximum
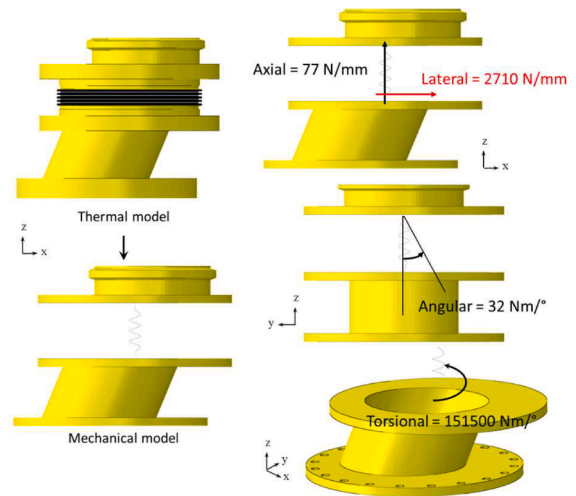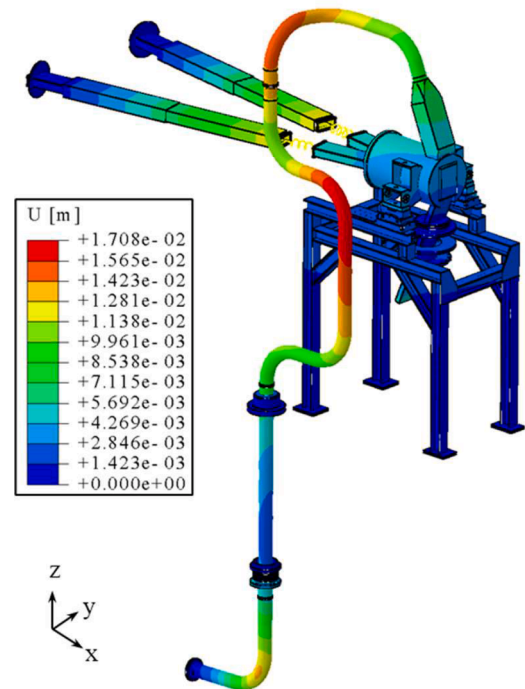

Fig. 10. ON bellows mechanical modelling.

Fig. 11. Displacement field within TSY.
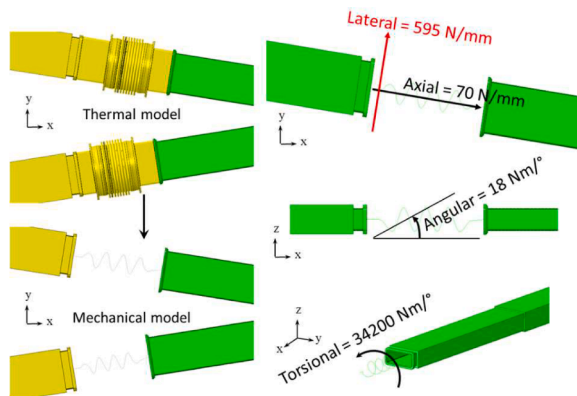

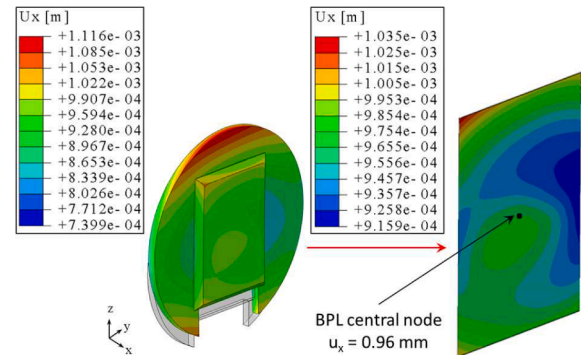**Fig. 9.** BDs bellows mechanical modelling.

Fig. 12. BPL displacements along X direction and focus on the surface closest to the HFTM.

Table 1

BDs and ON bellows relative displacements.

	Axial displacement [m]	Lateral displacement [m]
BDs bellow Yneg	$\Delta U\gamma = 9.21\text{E-}03$	$\|\Delta U\theta_1\| = 6.22\text{E-}04$
		$\|\Delta U\theta_2\| = 1.46\text{E-}02$
BDs bellow Ypos	$\Delta U\gamma = 9.30\text{E-}03$	$\|\Delta U\theta_1\| = 5.01\text{E-}04$
		$\|\Delta U\theta_2\| = 1.46\text{E-}02$
ON bellow	$\Delta U\gamma = -9.89\text{E-}04$	$\|\Delta U\theta_1\| = 1.90\text{E-}03$
		$\|\Delta U\theta_2\| = 5.24\text{E-}04$

displacement of ~3.6 mm is predicted, the risk of contact can be excluded.

4. TSY transient thermo-mechanical analysis

In order to assess the transient thermo-mechanical behaviour of the DONES TSY under the start-up loading scenario, a campaign of analysis has been carried out. The considered scenario can be divided in two phases. The first one is the pre-heating phase, in which no lithium flows inside the TSY and a set of electric heaters, located onto the external surfaces of different regions, acts with a proper duty cycle with aim of increasing as evenly as possible the temperature of the structure. The second phase, the lithium flow phase, starts after the pre-heating and envisages that the lithium enters the TSY at 300 °C. In particular, the analysis considering 6 h of pre-heating phase and 12 h og lithium flow phase are here reported.

4.1. Thermal analysis: the 3D fem model

In order to perform the transient thermal analysis of the DONES TSY under the transient start-up loading scenario, the geometric configuration already adopted for the steady state calculations has been used. Hence, the 3D FEM model has been inherited from steady state analysis and properly adapted to the transient calculations. A uniform TSY initial temperature of 50 °C has been imposed for the transient analysis, considering the TSY in equilibrium with the TC atmosphere prior to the beginning of the pre-heating phase.

Since the pre-heating phase is characterized by the absence of Li and the action of a set of electric heaters located onto the TSY external surfaces, the following loads and boundary conditions have been considered:

- time-dependant heat fluxes from electric heaters;
- thermal contacts modelling;
- external and internal TAA uninsulated surfaces heat transfer;
- imposed temperatures.

The reference TSY pre-heating procedure has been adopted for the analysis here reported [4]. The surfaces of action of the electric heaters and the heat fluxes exerted by them when they are switched on [4] are shown in Fig. 13. As one can see, heaters have been supposed to be located onto Outlet Nozzle (ON), Target Vacuum Chamber (TVC), Inlet Nozzle (IN), bend Inlet Pipe (IP bend), straight Inlet Pipe (IP straight), upper and lower Joint (Joint up and Joint down) [4].

Then, in order to ensure a TSY pre-heating as even as possible and, at the same time, achieving quite high Li channel temperatures, a pre-heating phase duration of 12 h has been initially assumed with the heaters reference duty cycle [4]. Since preliminary results have shown that such a pre-heating duration is excessive in terms of stress amount, the duration has been halved. For the sake of brevity, those results have not been reported here.

The remaining loads and boundary conditions, listed above, applied during the pre-heating phase are similar as those described in §3.1 but considering the absence of the lithium inside the TSY.

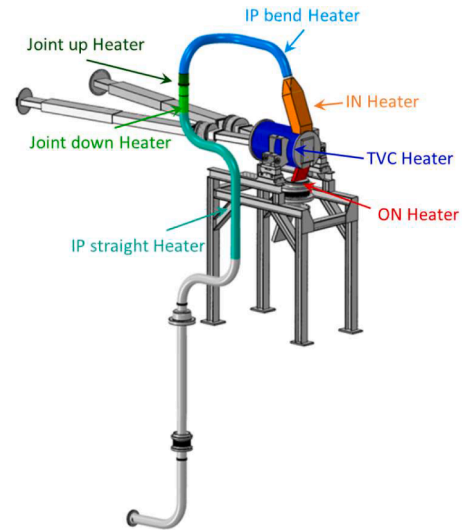As to the lithium flow phase, it begins just after the conclusion of the

Fig. 13. Electric heaters surfaces and corresponding heat fluxes.

pre-heating, the latter lasting for 6 h Hence, no electric heater is acting anymore in this phase. Instead, lithium enters the TSY at 300 °C. The following loads and boundary conditions have been considered in this phase:

- thermal contacts modelling;
- external and internal TAA uninsulated surfaces heat transfer;
- imposed temperatures;
- lithium flow convective heat transfer.

Details of the above mentioned loads and boundary conditions can be found in §3.1. In particular, the start of the lithium flow has been simulated switching off/on the contact between the lithium convective elements and the structure.

4.1. Thermal analysis: results.

A transient analysis foreseeing a pre-heating phase lasting for 6 h followed by a lithium inlet phase of 24 h has been carried out. In Figs. 14 and 15, the thermal field arising within the BPL at different time steps of both phases are reported.
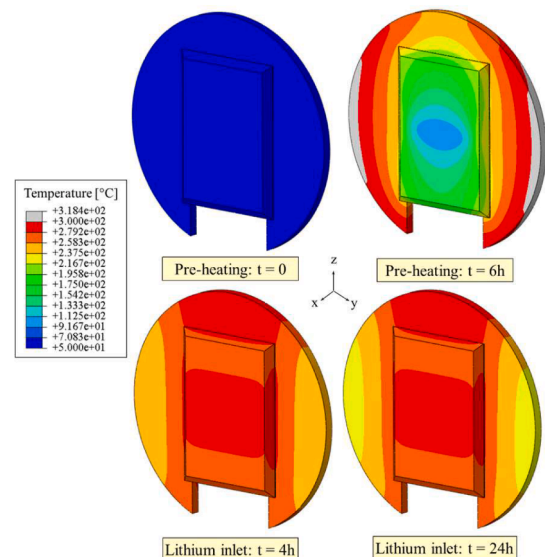

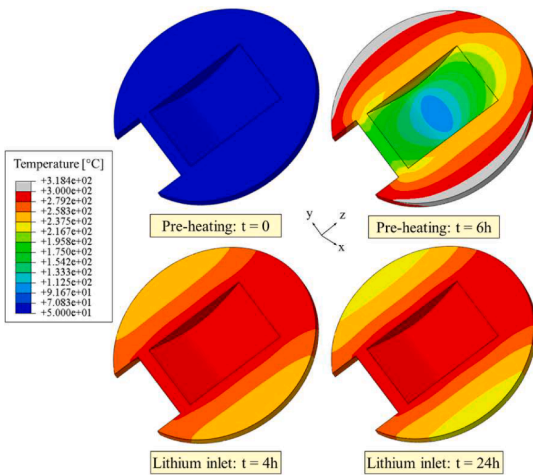**Fig. 14.** Transient analysis: BPL thermal field - view1.

Fig. 15. Transient analysis: BPL thermal field - view2.

Moreover, the minimum temperature of the lithium domain in the first 60 s is reported in Fig. 16. As can be observed, the lithium temperature never falls below 200 °C and after about 20 s it starts to stabilise around 300 °C. This outcome ensures that lithium does not reach the limit temperature of 200 °C (equal to the lithium melting temperature plus a 10% margin) [4], below which its freezing may occur.

Moreover, in Figs. 17 and 18, the maximum temperature achieved onto the TSY surfaces housing the heaters and of the lithium-wetted BPL and ON surfaces are reported. As it can be observed, the maximum temperature reached on the surfaces ranges between 400 °C and ~250 °C. Just on the external surface in correspondance of the TVC heater, 550 °C is slightly exceeded at the end of the pre-heating phase. In this regard, a revision of the heaters duty-cycle would be helpful and it could also improve the structural performances. Instead, the chart showing the maximum temperature during the lithium inlet phase is truncated at 10 h because after 9 h the maximum temperatures converge around 300 °C.

4.2. Structural analysis: the fem model

Once assessed the thermal transient behaviour of the DONES TSY under the start-up scenario, a series of static structural analyses have been performed at the most significant time steps in order to assess its structural response in view of the RCC-MRx code.

The same mesh and the same set of loads and boundary conditions already presented in §3.3 have been adopted, with the necessary modifications in the pre-heating phase since it is characterized by no lithium flow.
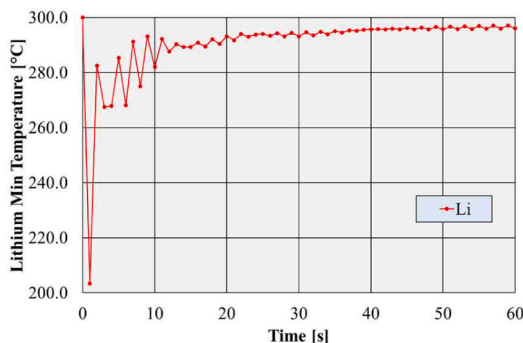

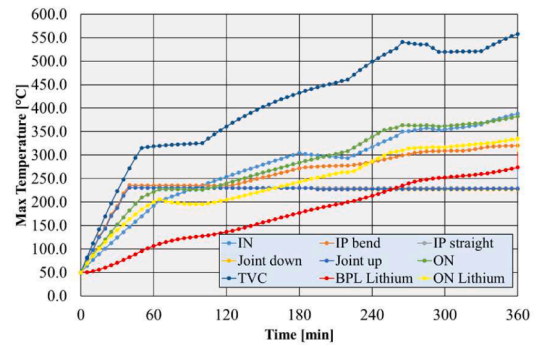**Fig. 16.** Transient analysis: Minimum lithium temperature.

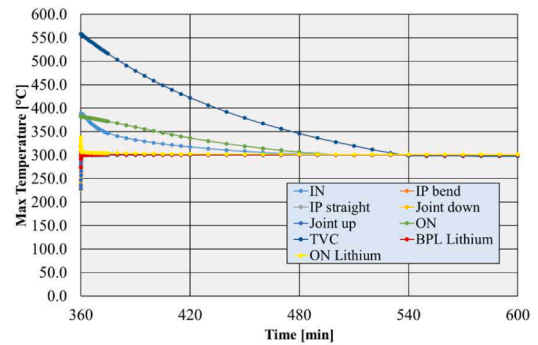**Fig. 17.** Pre-heating phase: Maximum temperature of the ON, BPL and heaters external surfaces.

Fig. 18. Lithium inlet phase: Maximum temperature of the ON, BPL and heaters external surfaces.

4.3. Structural analysis: results

Since the most critical region of the TSY is the BPL, for the sake of brevity only the arising Von Mises stress field within it is reported in Figs. 19 and 20 in some significan time steps. Results show that at the end of pre-heating the highest stress is achieved in correspondance of
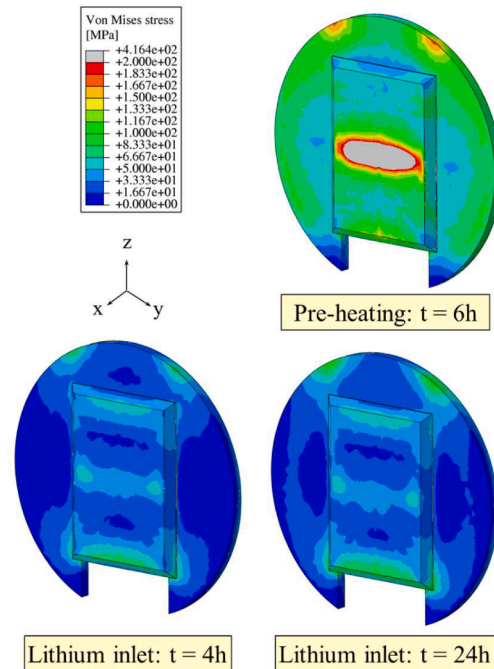

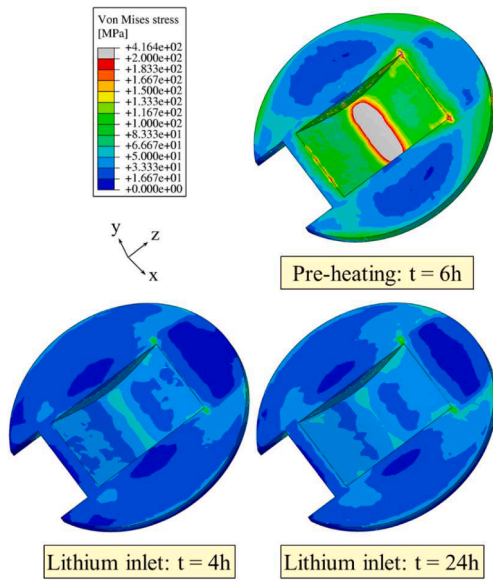**Fig. 19.** BPL Von Mises stress field - view1.

Fig. 20. BPL Von Mises stress field - view2.

the BPL lowest thickness.

Then the fulfilment of the RCC-MRx design criteria have been checked. In particular, four criteria have been taken into account: Immediate Excessive Deformation (IED), Immediate Plastic Instability (IPI), Immediate Plastic Flow Localization (IPFL) and Immediate Fracture due to exhaustion of ductility (IF). The selected criteria are reported in Table 2, where S_m is the maximum allowable primary membrane stress intensity of the material, S_{em} is the maximum allowable primary plus secondary membrane stress, function of temperature, S_{et} is the maximum allowable total stress, also function of temperature, and, finally, K_{eff} is a factor called "plastic collaboration coefficient", equal to 1.5 for rectangular sections. Temperature-dependant values of S_m, S_{em} and S_{et} have been calculated according to the structural material Eurofer properties.

Looking at the Von Mises equivalent stress field, different paths have been selected within the BPL in correspondance of its most stressed regions. In particular, in Fig. 21 the localization of the BPL paths is reported. In correspondance of each marked point, a path has been indentified along the corresponding BPL thickness.

For the sake of brevity, only the results of the verification of the IPFL criteria for each path and for every time-step have been reported in Fig. 22. In fact, the other criteria are fully met along all the paths. The correspondance between the steps shows in Fig. 22 and the time istants is reported in Table 3.

Conversely, looking at the results of the verification of the criterion taking into account also the secondary loads (IPFL), it can be noticed that from the time step 20, which refers to the time step equal to 4h25min during the pre-heating phase, to the time step 24, i.e. the end of that phase, some paths located in the middle region of the BPL do not fulfil the criterion. In any case, this behaviour appears not particularly

Table 2
RCC-MRx design criteria.

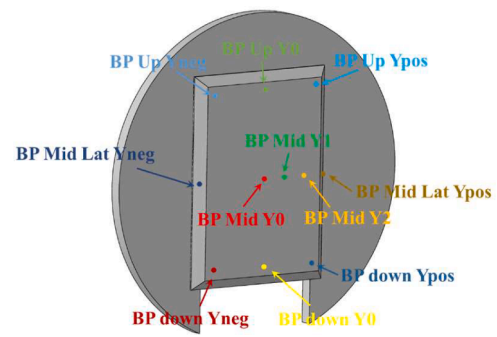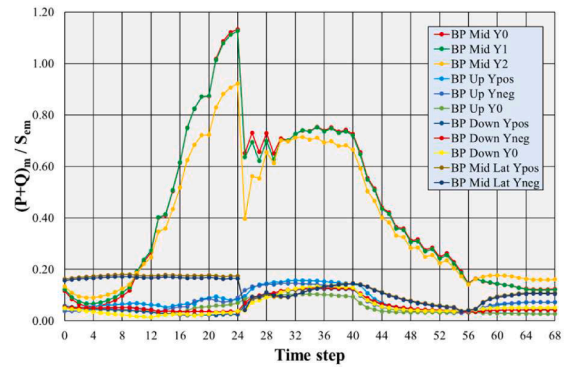|	Criteria
Immediate Excessive Deformation	$\dfrac{P_m}{S_m} < 1$
Immediate Plastic Instability	$\dfrac{P_m + P_b}{K_{eff} \cdot S_m} < 1$
Immediate Plastic Flow Localization	$\dfrac{P_m + Q_m}{S_{em}} < 1$
Immediate Fracture due to exhaustion of ductility	$\dfrac{P_m + P_b + Q + F}{S_{et}} < 1$

Fig. 21. BPL selected paths.

Fig. 22. Immediate plastic flow localization criterion results.

Table 3
Step-time correspondence.

Pre-heating phase		Lithium flow phase	
Step	Time	Step	Time
0	5min	28	4s
4	25min	32	20s
8	45min	36	40s
12	65min	40	1min
16	3h	44	5min
20	4h25min	48	9min
24	6h	52	13min
		56	45min
		60	4h
		64	12h
		68	24h

worrying because the criterion is slighly not fulfilled and, globally, the BPL shows a good structural behaviour. Moreover, the application of other methodology not as conservative as the elastic route, and even more realistic, might yield to enough margin.

Some design improvement is needed but this is not expected to represent a big concern. In fact, on the one hand, it might be possible to reduce the pre-heating phase to 4h25min, but, on the other hand, it is not certain that the Lithium temperature will remain above 200 °C.

5. Conclusion

A research campaign has been performed to assess the thermal and structural performances of the latest geometric layout of the DONES TSY under nominal steady state and transient start-up loading scenarios.

Steady state thermal analyses have shown that the maximum temperature is well below the Eurofer maximum allowable temperature, equal to 550 °C. From the structural standpoint, the BPL displacement are compliant with the minimum gap present between it and the HFTM,

whereas the prediction of the relative displacement of the flanges connected by the bellow will help in qualifying their design. Transient analysis allowed concluding that, adopting the reference heaters duty cycle, after 6 h of pre-heating the lithium can enter and its minimum temperature remains above 200 °C. This implies that the insurgence of high stress is only in a very localised region, where the RCC-MRx criteria are not totally fulfilled even if with a narrow margin.

Globally, results of the thermo-mechanical analysis are promising but minor modifications are still needed to improve the TSY behaviour. In particular, the analysis showed the necessicity to include the proper supports for the BDs in the FEM model, to simulate the connection between the TAA and the HFTM more in detail, to further improve the pre-heating procedure and to relax the conservatism in the application of some RCC-MRx criteria. Further analyses are ongoing in order to obtain an higher temperature (about 200 °C) at the Lithium channel centre.

CRediT authorship contribution statement

I. Catanzaro: Data curation, Formal analysis, Investigation, Methodology, Resources, Validation, Visualization, Writing – original draft, Writing – review & editing. **P. Arena:** Conceptualization, Data curation, Investigation, Methodology, Resources, Visualization, Writing – review & editing. **D. Bernardi:** Conceptualization, Data curation, Investigation, Methodology, Resources, Visualization, Writing – review & editing. **G. Bongiovì:** Conceptualization, Data curation, Formal analysis, Investigation, Methodology, Resources, Validation, Visualization, Writing – original draft, Writing – review & editing. **T. Dezsi:** Conceptualization, Data curation, Investigation, Methodology, Resources, Visualization, Writing – review & editing. **P.A. Di Maio:** Conceptualization, Data curation, Funding acquisition, Investigation, Methodology, Project administration, Resources, Supervision, Visualization, Writing – review & editing. **F.S. Nitti:** Conceptualization, Data curation, Investigation, Methodology, Resources, Visualization, Writing – review & editing. **S. Giambrone:** Conceptualization, Data curation, Formal analysis, Investigation, Methodology, Resources, Visualization, Writing – original draft, Writing – review & editing. **M. Giardina:** Conceptualization, Data curation, Investigation, Methodology, Resources, Visualization, Writing – review & editing. **S. Gordeev:** Conceptualization, Data curation, Investigation, Methodology, Resources, Visualization, Writing – review & editing. **A. Quartararo:** Conceptualization, Data curation, Investigation, Methodology, Resources, Visualization, Writing – review & editing. **E. Tomarchio:** Conceptualization, Data curation, Investigation, Methodology, Resources, Visualization, Writing – review & editing. **E. Vallone:** Conceptualization, Data curation, Investigation, Methodology, Resources, Visualization, Writing – review & editing.

Declaration of competing interest

The authors declare that they have no known competing financial interests or personal relationships that could have appeared to influence the work reported in this paper.

Data availability

No data was used for the research described in the article.

References

[1] D. Bernardi, et al., The IFMIF-DONES Project: design Status and Main Achievements within the EUROfusion FP8 Work Programme, J. Fus. Ener. 41 (2022) 24, https://doi.org/10.1007/s10894-022-00337-5.

[2] W. Królas, et al., The IFMIF-DONES fusion oriented neutron source: evolution of the design, Nucl. Fus. 61 (2021) 125002, https://doi.org/10.1088/1741-4326/ac318f.

[3] P. Arena, et al., The design of the DONES lithium target system, Fus. Engineer. Des. 146 (2019) 1135–1139, https://doi.org/10.1016/j.fusengdes.2019.02.024, part A.

[4] P. Arena, et al., Determination of a pre-heating sequence for the DONES Target Assembly, Fus. Engineer. Des. 168 (2021) 112394, https://doi.org/10.1016/j.fusengdes.2021.112394.

[5] RCC-MRx, Design and Construction Rules For Mechanical Components of Nuclear Installations, AFCEN, Courbevoie, France, 2013.

[6] Abaqus Analysis User's Guide: Online Documentation; Version 6.14-2; Dassault System, Simulia, Providence, RI, USA, 2015.

[7] E. Gaganidze, Material Properties Handbook – EUROFER97, IDM Ref.: 2NZHBS, 2020. https://idm.euro-fusion.org/?uid=2NZHBS.

[8] P.D. Desai, C.Y. Ho, Thermal Linear Expansion of Nine Selected AISI Stainless Steels, CINDAS report for the American iron and steel institute, April 1978.

[9] Engineering Properties At Elevated Temperatures, International Nickel Company databooks, 1963.

[10] E.I. Gol'tsova, Densities of Lithium, Sodium, and Potassium at temperatures up to 1500-1600°C, High Temp. 4 (1966) 348.

[11] E.E. Shpil'rain, I.F. Krainova, Measurement of the thermal conductivity of liquid lithium, High Temp. 8″ (1970) 1036–1038.

[12] J.W. Cooke, Experimental Determination of the Thermal Conductivity of Molten Lithium from 320° to 830 °C, J. Chem. Phys. 40 (1964) 1902.

[13] A. Serikov, Nuclear heating inside the IFMIF-DONES Test Cell, target assembly, and their components. http://idm.euro-fusion.org/?uid=2PKZRA.

[14] A. Tincani, D. Bernardi, G. Miccichè, Engineering design report of the EVEDA bayonet concept Back-Plate, ENEA Report IM-M-R-002, 04/02/2010.

[15] P. Arena, et al., Thermomechanical analysis supporting the preliminary engineering design of DONES target assembly, Fus. Engineer. Des. 136 (2018) 1332–1336, https://doi.org/10.1016/j.fusengdes.2018.05.003.

[16] N. Uda, et al., Forced convection heat transfer and temperature fluctuations of lithium under transverse magnetic fields, J. Nucl. Sci. Technol. 38 (2001) 936–943, https://doi.org/10.1080/18811248.2001.9715120.

[17] M. Rosenberg, et al., On thermal radiation from fusion related metals, Fus. Engineer. Des. 84 (1) (2009) 38–42, https://doi.org/10.1016/j.fusengdes.2008.08.046.

[18] P.A. Di Maio, et al., Study of the thermo-mechanical performances of the IFMIF-EVEDA Lithium Test Loop target assembly, Fus. Engineer. Des. 87 (5–6) (2012) 822–827, https://doi.org/10.1016/j.fusengdes.2012.02.030.

[19] F.P. Incropera, D.P. De Witt, Fundamentals of Heat and Mass Transfer, 4th Edition, John Wiley & Sons, 1996.

[20] F.S. Nitti, State of Pressure in TA and TC (Update, table) (2018). http://idm.euro-fusion.org/?uid=2N7GAB.

[21] F. Schwab, FTM upgrade of conceptual design alternatives (2018), http://idm.euro-fusion.org/?uid=2MUEU3.

[22] G. D'Ovidio, Lithium level estimation in the Quench Tank concept with flat walls (2020), http://idm.euro-fusion.org/?uid=2NBKFP.

[23] S. Gordeev, Update calculation of the temperature distribution in the Li and in the TAA, structure (2021). http://idm.euro-fusion.org/?uid=2NVVUN.

[24] A. Serikov at, et al., Thermo-mechanical update of the TAS for the reference beam, footprints (2023). https://idm.euro-fusion.org/?uid=2QKU5D.

[25] V. Pierantoni, Heat Removal System DDD- version 2021 (2021), http://idm.euro-fusion.org/?uid=2NQYJD.

[26] T. Dézsi, 2021 EK-CER Industry contribution to the design of the HFTM supporting structure (2022), http://idm.euro-fusion.org/?uid=2PDWMR.